ARCHIVES OF CIVIL ENGINEERING, LVII, 2, 2011

DOI: 10.2478/v.10169-011-0017-1

THE INFLUENCE OF SELECTED MATERIAL AND TECHNOLOGICAL FACTORS ON MECHANICAL PROPERTIES AND MICROSTRUCTURE OF REACTIVE POWDER CONCRETE (RPC)

T. ZDEB[1], J. ŚLIWIŃSKI[2]

The paper deals with the properties and microstructure of Reactive Powder Concrete (RPC), which was developed at Cracow University of Technology. The influence of three different curing conditions: water (W), steam (S) and autoclave (A) and also steel fibres content on selected properties of RPC was analyzed. The composite characterized by w/s ratio equal to 0.20 and silica fume to cement ratio 20%, depending on curing conditions and fibres content, obtained compressive strength was in the range from 200 to 315 MPa, while modulus of elasticity determined during compression was about 50 GPa. During three-point bending test load-deflection curves were registered. Base on aforementioned measurements following parameters were calculated: flexural strength, stress at limit of proportionality (LOP), stress at modulus of rapture (MOR), work of fracture (WF), and toughness indices I_5, I_{10} and I_{20}. Both amount of steel fibres and curing conditions influence the deflection of RPC during bending.

Key words: reactive powder concrete, ultra high performance cementitious composites, steel fibres, fibres volume ratio, curing conditions, strength, fracture energy, fracture toughness index.

1. Introduction

According to Collepardi, [6] dispersed reinforcement in reactive powder concretes is a standard component. Amongst the RPC composites the most recognized materials are the ones containing steel fibres. Fundamental aims for steel fibres application are: enhancing of mechanical properties, reduction of the shrinkage and inducing ductility of loaded material. The mean length of steel fibres in RPC ranges from 6 to 15 mm and diameter from 0.16 to 0.18 mm, while the volumetric content varies from 2.0 to 2.5% [15]. Characteristics of compressive and tension strength of RPC composites with constant amount of fibres are described among the others in the papers [1,3,9,12,17]. However, it is difficult to find some information on influence of variable content of the fibres with constant geometrical parameters on mechanical properties of reactive powder concretes.

[1] Cracow University of Technology, Faculty of Civil Engineering, Warszawska 24, 31-155 Kraków, Poland, e-mail: tzdeb@pk.edu.pl; jsliwins@imikb.wil.pk.edu.pl

Hydrothermal curing conditions are also of great importance in development of mechanical properties of reactive powder concretes [6,18]. Steam curing increases both compressive and flexural strengths, but also influence on other properties like microporosity [5,9] or shrinkage [16]. However, primary setting time in natural condition has to be suitable, in order to prevent delayed ettringite formation [11]. Autoclaving also improves many features of cementitious composites, especially mechanical properties [15]. This can be attributed to enhancement of pozzolanic activity of ingredients as well as presence of crystalline forms of hydrated calcium silicates [13].

2. Materials and specimen preparation

2.1. Materials

In order to produce RPC specimens, following components were used: portland cement CEM I 52.5R, silica fume, ground quartz 0/0.2 mm, quartz sand 0/0.5 mm, common acrylic-based superplasticizer and straight, smooth steel fibres. Detailed characteristics of applied materials are presented in Tables 1÷4.

Table 1

Properties, chemical and phase composition of cement CEM I 52.5R.
Fizyczne i chemiczne właściwości cementu CEM I 52,5R

Properties	
Initial setting time [min]	130
Final setting time [min]	220
Specific surface [cm^2/g]	4100
compressive strength after 2 days [MPa]	34.5
compressive strength after 28 days [MPa]	70.8
Chemical composition [weight %]	
CaO – 65.58; SiO_2 – 22.98; Al_2O_3 – 4.41; Fe_2O_3 – 2.10; SO_3 – 3.32; MgO – 1.06; Na_2O_E – 0.51; Cl^- - 0.009	
Phase composition [weight %]	
C_3S – 59.09; C_2S – 17.97; C_3A – 8.12; C_4AF – 6.38	

2.2. Composition of RPC matrix

Composition of examined RPC was developed in the other research project, described in detail in [13]. Mix proportions are presented in Table 5. The maximum volume fraction of steel fibres (V_{fmax} = 4% vol.) was defined by obtaining proper workability of the concrete mixture without changing its composition and assumption that inclusion is homogeneously dispersed within the whole composite.

Table 2

Particle size distribution and chemical composition of ground quartz and sand.
Charakterystyka uziarnienia i składu chemicznego mączki kwarcowej oraz piasku

Properties	**Ground quartz**	**Sand**
D_{max} [μm]	200	500
D_{50} [μm]	16	110
Specific surface BET [m^2/g]	0.8	0,04
Density [g/cm^3]	2.65	
Polimorfic modification	β−quartz	
SiO_2 [%]	99.0	98.5
Al_2O_3[%]	0.3	0.8
Fe_2O_3[%]	0.05	0.03

Table 3

Selected properties and chemical composition of silica fume.
Wybrane właściwości i skład chemiczny pyłu krzemionkowego

Properties	
Specific surface [m^2/g]	22.4
Density [g/cm^3]	2.23
Chemical composition [% w.]	
SiO_2– 94.06; Al_2O_3 – 0.74; Fe_2O_3 – 0.78; CaO – 0.06; MgO – 0.49; Na_2O_e – 1.43; SO_3 – 0.63; Loss On Ignition – 0.74	

Table 4

Steel fibres properties.
Właściwości włókien stalowych

Length [mm]	6
Diameter [mm]	0.175
Modulus of elasticity [GPa]	210
Tensile strength [MPa]	2200

Table 5

Composition of RPC matrix by weight ratio.
Skład mineralnej matrycy RPC (proporcje masowe)

Cement CEM I 52,5R	1.00
Silica fume	0.20
Grounded quartz 0/0,20 mm	0.34
Quartz sand 0/0,50 mm	0.81
Superplasticizer	0.02
Water	0.24

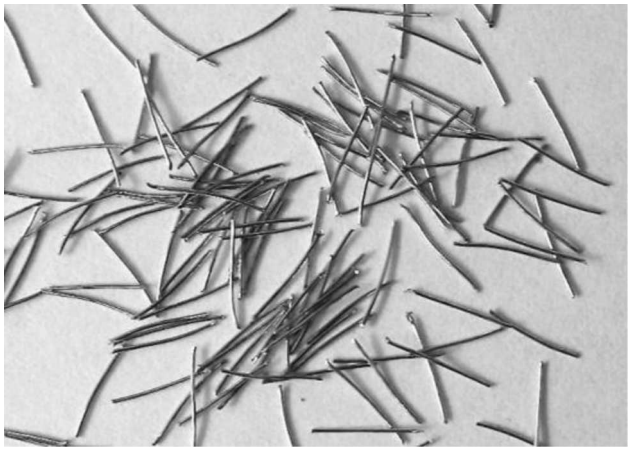

Fig. 1. Picture of applied steel fibres (l = 6 mm; ϕ = 0.16 mm).
Rys. 1. Wygląd zastosowanych włókien stalowych (l = 6 mm; ϕ = 0,16 mm)

Above-mentioned mixture includes following amount of steel fibres: V_f = 0.5; 1.0; 2.0; 3.0 and 4.0% vol. (i.e. 39, 78, 155, 233 and 310 kg/m^3).

2.3. Specimens and curing conditions

The mixtures with fibres were molded and compacted in gravitational manner. Preliminary setting of concretes lasted for 6 or 24 hours at +20°C, during this time evaporation of water was prevented. After demoulding the specimens were cured under three different conditions:

- curing in water at +20°C after 24 hours of preliminary setting (W),
- steam curing at +90°C after 6 hours of preliminary setting, according to cycle presented in Fig. 2 (S),
- autoclaving at +250°C and under pressure of 40 bars after 24 hours of preliminary setting, according to cycle presented on Fig. 2 (A).

3. Procedures and test results

3.1. Compressive strength

The compressive strength of each material was obtained by testing 12 cubes (40×40×40 mm). The specimens were cut from beams with dimensions 40×40×160 mm. Regardless of steel fibres amount, the cross section confirmed, that each specimen has quasihomogeneous fibres dispersion (see Fig. 3).

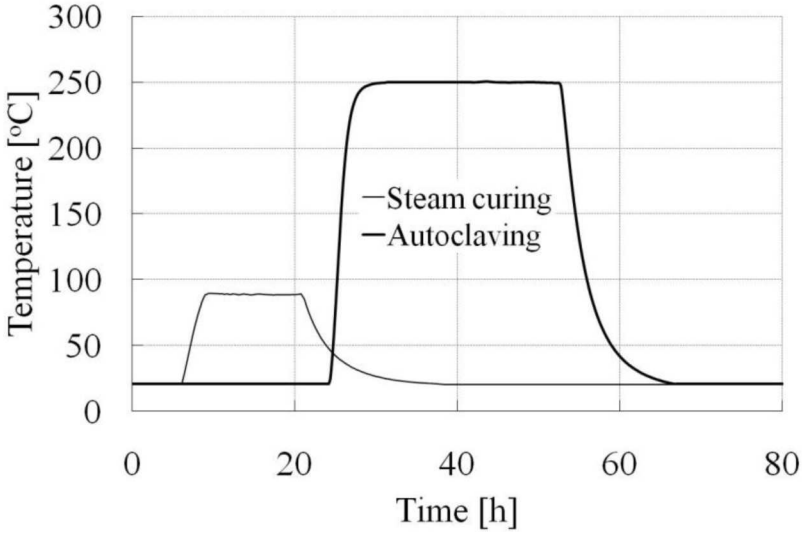

Fig. 2. Temperature versus time for autoclaving and steam curing.
Rys. 2. Zmienność temperatury w czasie autoklawizacji i niskoprężnego naparzania

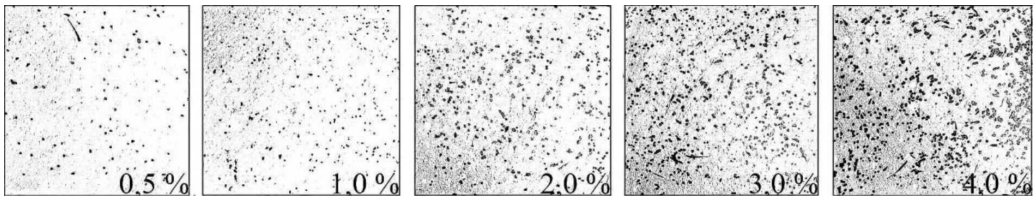

Fig. 3. The cross section of tested beams with quasihomogeneously dispersed steel fibres.
Rys. 3. Przekroje badanych beleczek z quasihomogenicznym rozkładem włókien stalowych

Table 6 includes average values of compressive and flexural strengths. In case of curing in water (W), specimens were examined after 28 days of setting. Steam cured (S) and autoclaved (A) specimens were tested after heat treatment was completed and the specimens were cooled down.

3.2. Deformability during compression

Deformability of each composite was determined on three cylindrical specimens with dimensions 50×100mm. Six electric resistance wire strain gauges with the length of measurement equal to 15mm and nominal resistance 120Ω were stuck on the specimens. Three of them were placed in order to measure transverse deformation ε_x and the other three for longitudinal deformation ε_y, (see Fig. 4). Modulus of elasticity was determined according to procedure which is characterized in PN-EN 14580 [14].

Table 6

Compressive and flexural strength of RPC with and without steel fibres, cured in three different hydrothermal conditions.
Wytrzymałość na ściskanie i rozciąganie przy zginaniu RPC z oraz bez włókien stalowych, dojrzewających w trzech różnych warunkach hydrotermalnych

Curing conditios	Without fibres [MPa]	Variable volume fraction of fibres [% vol.]				
		0.5	1.0	2.0	3.0	4.0
W	194	202	201	208	211	217
S	212	219	215	224	228	235
A	268	282	281	297	308	315

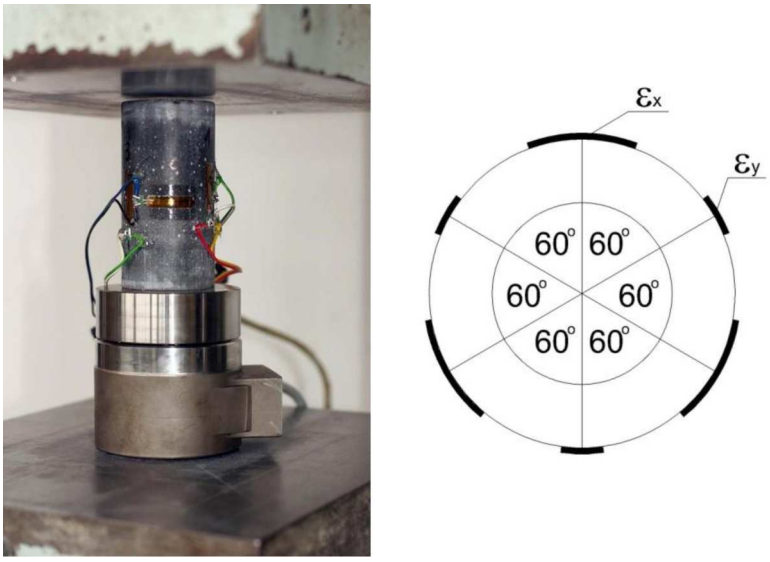

Fig. 4. Specimen of the RPC prepared for determination of deformability during compression and scheme of electric resistance wire strain gauges arrangement.
Rys. 4. Próbka RPC przygotowana do oznaczenia odkształcalności podczas ściskania wraz ze schematem rozkładu tensometrów elektrooporowych

The test of deformability during compression was developed for following materials: samples without steel fibres cured in water (W), steam-cured (S), autoclaved (A) and for composite, which contains maximum amount of fibres (4% vol.) cured in autoclave (ASt). Aforementioned choice of composites was made in order to obtain an information about the influence of curing conditions and presence of steel fibres on deformability of RPC. The test results as a relation between stress and deformation are presented in the Fig. 5.

On the basis of curves registered $\sigma - \varepsilon_x$ and $\sigma - \varepsilon_y$, values of both modulus of elasticity and Poisson ratio were calculated for four different variants of RPC composites (see Table 7).

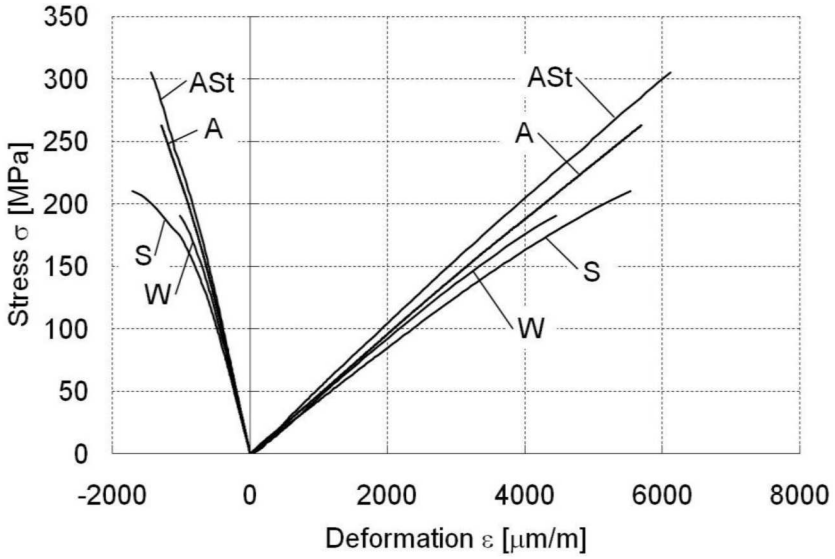

Fig. 5. Longitudinal and transverse deformation versus compressive stress.
Rys. 5. Zależności pomiędzy naprężeniem ściskającym a odkształceniem podłużnym i poprzecznym

Table 7

Average values of modulus of elasticity and Poisson ratio for selected variants of RPC composites.
Średnie wartości modułu sprężystości i współczynnika Poissona różnych wariantów kompozytów RPC

Composite	Modulus of elasticity [GPa]	Poisson ratio [-]
Without fibres – water 20°C (W)	47	0,20
Without fibres – steam-curing 90°C (S)	44	0,20
Without fibres – autoclaving 250°C (A)	50	0,21
Steel fibres V_f=4% vol. – autoclaving 250°C (ASt)	50	0,20

3.3. Flexural strength

In order to determine flexural strength, three-point bending test and the specimens with dimensions 40×40×160 mm were applied. The distance between supports was equal to 100 mm. Loading of the specimen was determined by force gain. The terms of flexural strength tests was analogous to aforementioned compressive strength measurements. Table 8 includes average values of flexural strengths of all considered materials.

3.4. Deformability during bending

Deformability of the specimens was registered during determination of flexural strength. Dimensions of the specimens and the rate of loading were not consistent with ASTM C1018-97 [2]. Therefore, the following analysis of calculated parameters has only

Table 8

Flexural strength of RPC with and without steel fibres, cured in three different conditions.
Wytrzymałość na rozciąganie przy zginaniu RPC z oraz bez włókien stalowych, dojrzewających w trzech różnych warunkach hydrotermalnych

Curing conditios	Without fibres [MPa]	Variable volume fraction of fibres [% vol.]				
		0.5	1.0	2.0	3.0	4.0
W	10.6	12.1	13.2	16.0	19.3	22.7
S	14.3	14.5	15.6	17.2	22.7	23.0
A	18.6	21.2	23.7	25.1	26.1	26.8

comparative character. Table 9 contains average values of toughness indices I_5, I_{10}, I_{20} and work of fracture WF computed as an area under whole load-deflection curve until the load equals zero. In order to determine appropriate volume fraction of steel fibres, that brings about deflection-hardening composite, the stress at LOP and MOR were calculated according to the following equation.

The LOP point is defined as the point where nonlinearity in the load–deflection curve becomes evident and the first crack of the matrix appears. Moreover the modulus of rapture (MOR) is defined as the point when softening of the composite starts to occur after the LOP point [7]. Aforementioned coefficients are also presented in the Fig. 6.

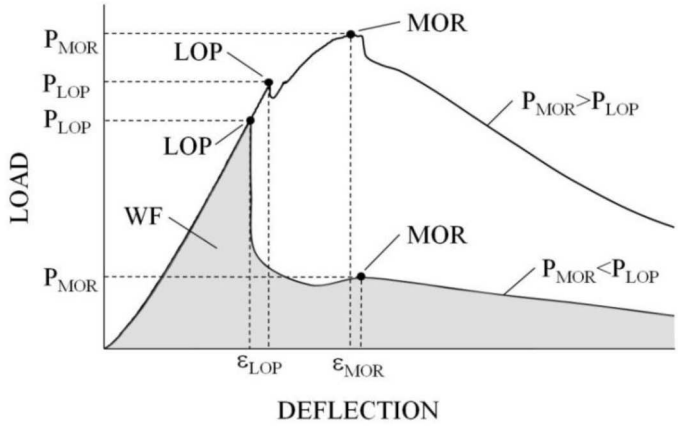

Fig. 6. Typical load-deflection curves of RPC containing steel fibres with determined coefficients.
Rys. 6. Typowe krzywe siła-ugięcie kompozytu RPC wraz z wyznaczanymi współczynnikami

Fig. 7 shows representative load-deflection relationship that were registered during studies. Both sides of the figure presents the same curves, however the difference concern the scale of deflection. On the right side of the figure the narrower scale was applied in order to highlight the limit of proportionality.

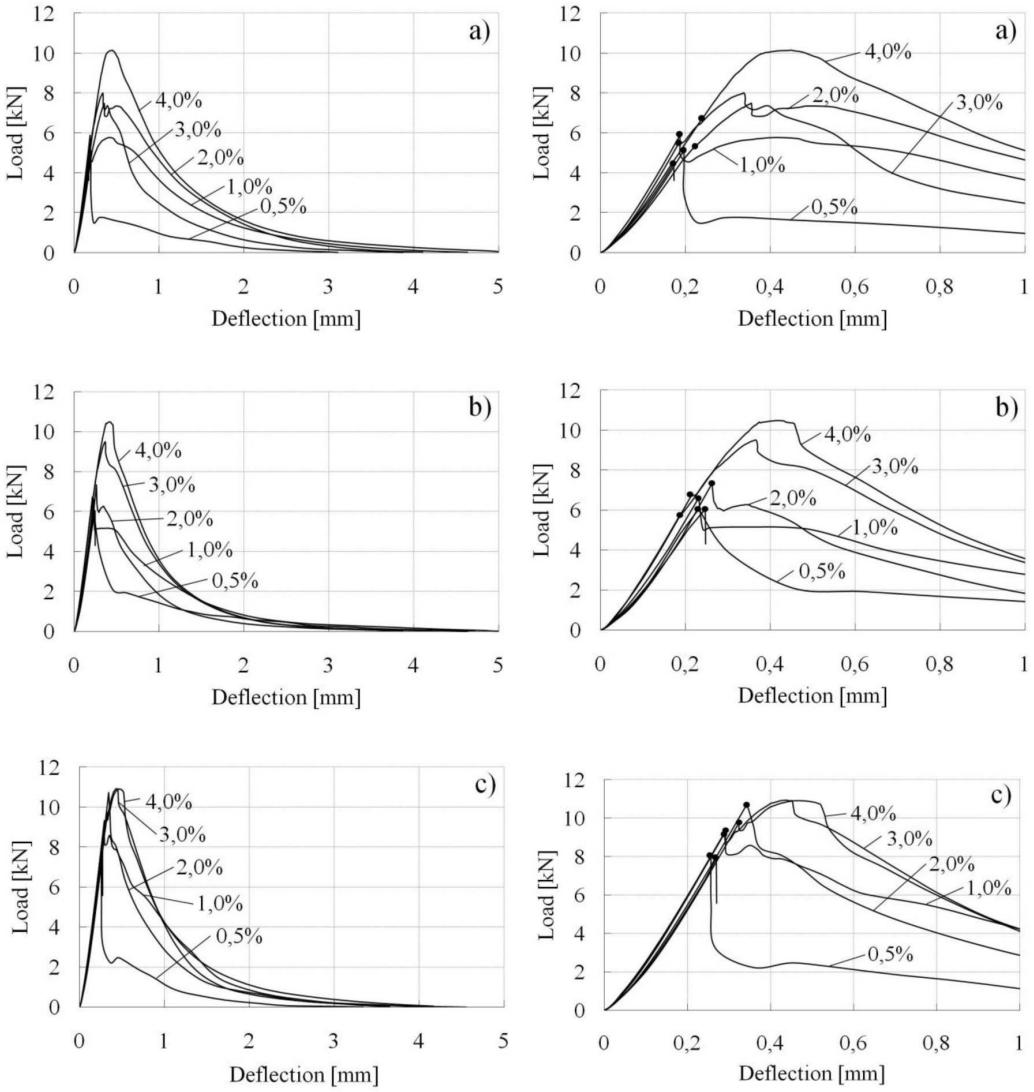

Fig. 7. Representative load-deflection curves registered during bending test of RPC with variable steel fibres content; a) setting in water, b) steam curing, c) autoclaving, (• – LOP).

Rys. 7. Reprezentatywne krzywe siła-ugięcie zarejestrowane podczas próby zginania RPC ze zmienną zawartością włókien; a) dojrzewanie w wodzie, b) niskoprężne naparzanie, c) autoklawizacja, (• – LOP)

Table 9

Average values of toughness indices I_5, I_{10}, I_{20}, work of fracture WF and stress at LOP and MOR.
Średnie wartości współczynników toughness indices I_5, I_{10}, I_{20}, energia zniszczenia WF oraz naprężenie w punktach LOP i MOR

Curing conditios	Features	Without fibres	Variable volume fraction of fibres [% vol.]				
			0.5	**1.0**	**2.0**	**3.0**	**4.0**
W	I_5 [-]	–	3.0	4.9	5.5	6.2	5.6
	I10 [-]	–	5.0	8.3	8.8	9.9	7.9
	I20 [-]	–	6.9	10.4	10.7	12.5	9.9
	WF [kNmm]	0.3	3.0	6.1	7.4	7.1	10.3
	f_{LOP} [MPa]	10.6	12.1	13.2	14.1	14.5	19.5
	f_{MOR} [MPa]	–	5.9	11.9	15.9	19.3	22.7
S	I_5 [-]	–	3.0	5.0	5.1	6.6	5.5
	I10 [-]	–	4.7	8.0	8.4	10.3	7.7
	I20 [-]	–	6.3	10.4	10.5	12.9	9.1
	WF [kNmm]	0.7	3.0	5.9	6.0	8.7	9.2
	f_{LOP} [MPa]	14.3	14.5	15.6	14.2	14.9	19.1
	f_{MOR} [MPa]	–	5.8	13.1	16.8	22.7	23.0
A	I_5 [-]	–	2.2	2.5	4.1	4.5	6.7
	I10 [-]	–	2.7	3.1	6.0	7.4	8.6
	I20 [-]	–	2.9	3.4	5.8	7.0	9.3
	WF [kNmm]	0.9	3.4	6.1	9.2	9.4	10.8
	f_{LOP} [MPa]	18.6	21.2	23.7	25.1	21.1	21.2
	f_{MOR} [MPa]	–	6.4	13.1	19.2	25.5	26.8

The values of work of fracture, toughness indices, stress at LOP and MOR versus fibres content are presented in Fig. 8. The point marked as ◯ on Fig. 8(e,f,g) shows estimated amount of steel fibres that brings about deflection-hardening behavior of composite during bending.

4. Microstructure of RPC

The influence of curing conditions and fibres content on compressive and flexural strength as well as deformability during bending can be explained by microstructure formation of tested materials. There are at least three factors that permit to obtain ultra-high performance cementitious composites:

– very compacted microstructure of CSH phase (Fig. 9),
– very good adhesion of CSH phase to mineral inclusions (grains of grounded quartz and quartz sand) and also to steel fibres (Fig. 10, 11 and 12),
– fill in voids in microstructure of materials caused by crystallization of xonotlite and tobermorite during autoclaving (Fig. 13).

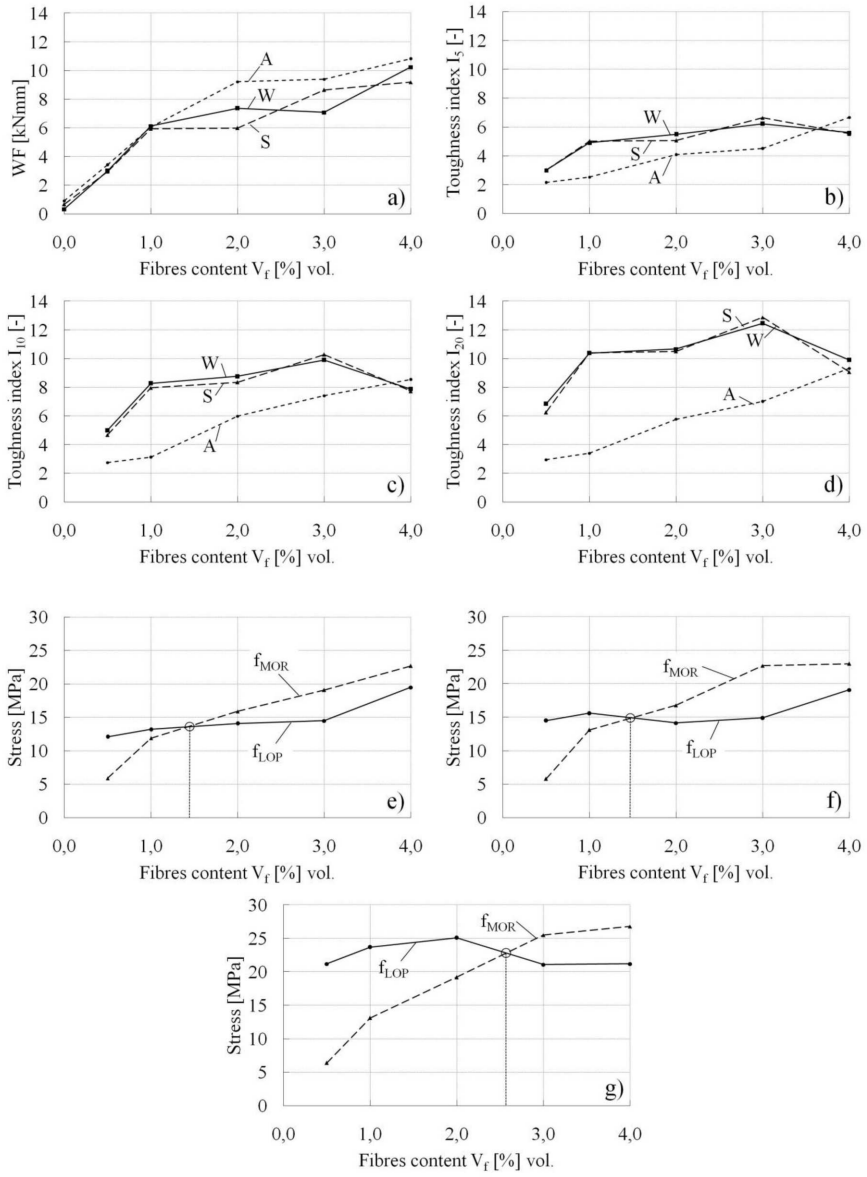

Fig. 8. Influence of curing conditions and fibres content on work of fracture WF (a), fracture toughness indices I_5, I_{10} , I_{20}, respectively (b, c, d) and stress at LOP and MOR for composites cured in water (e), steam-cured (f) and autoclaved (g).

Rys. 8. Wpływ warunków dojrzewania oraz zawartości włókien na energię zniszczenia WF (a), toughness indices I_5, I_{10}, I_{20}, odpowiednio (b, c, d) oraz na naprężenia w punktach LOP i MOR kompozytów RPC dojrzewających w wodzie (e), naparzanych (f) i autoklawizowanych (g)

Fig. 9 and 10 show microstructure formation of the composites cured in three different hydrothermal environments. Very compacted microstructure of CSH phase and its excellent adhesion to cement grains (light inclusion) as well as to quartz grains (dark inclusion) can be observed for each curing conditions. Steel fibres with tightly sheathed products of cement hydration are presented on Fig. 10, 11 and 12. Each voids of autoclaved RPC (pores, micro-cracking etc.) are completely or partly filled with crystals of xonotlite and tobermorite (Fig. 13).

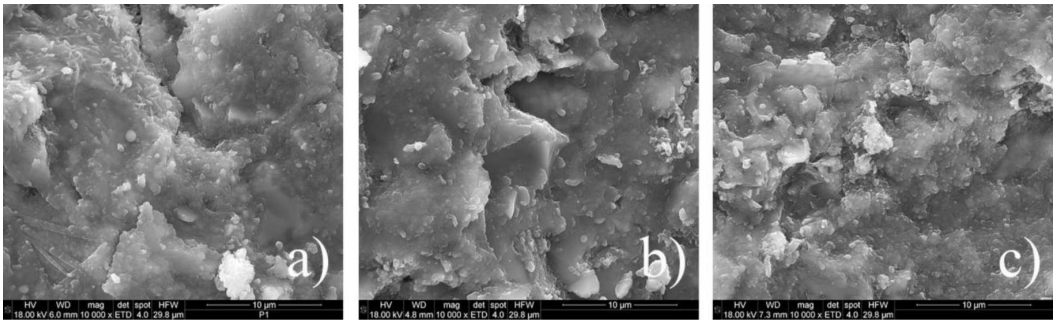

Fig. 9. CSH phase a) curing in water, b) steam curing, c) autoclaving, SEM, magnification 10000x.
Rys. 9. Faza CSH a) dojrzewanie w wodzie, b) naparzanie, c) autoklawizacja, SEM, powiększenie 10000x

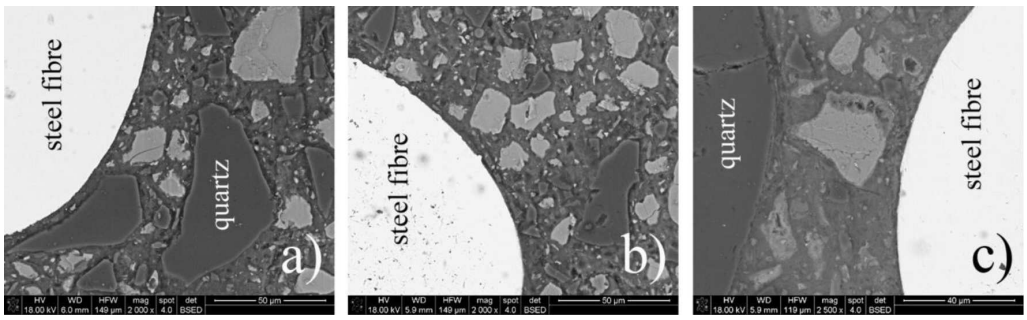

Fig. 10. Contact zone of steel fibre and CSH phase in RPC, a) curing in water, b) steam curing, c) autoclaving, SEM, magnification 2 000x.
Rys. 10. Strefa stykowa włókno stalowe - faza CSH w kompozytach RPC a) dojrzewających w wodzie, b) naparzanych, c) autoklawizowanych, SEM, powiększenie 2000x

In order to confirm influence of presence of xonotlite and tobermorite crystals on total microporosity of autoclaved composites, porosity distribution detected by mercury porosimetry was investigated. Fig. 14 presents relationship between pore volume and pore diameter of the RPC matrices cured in three considered conditions.

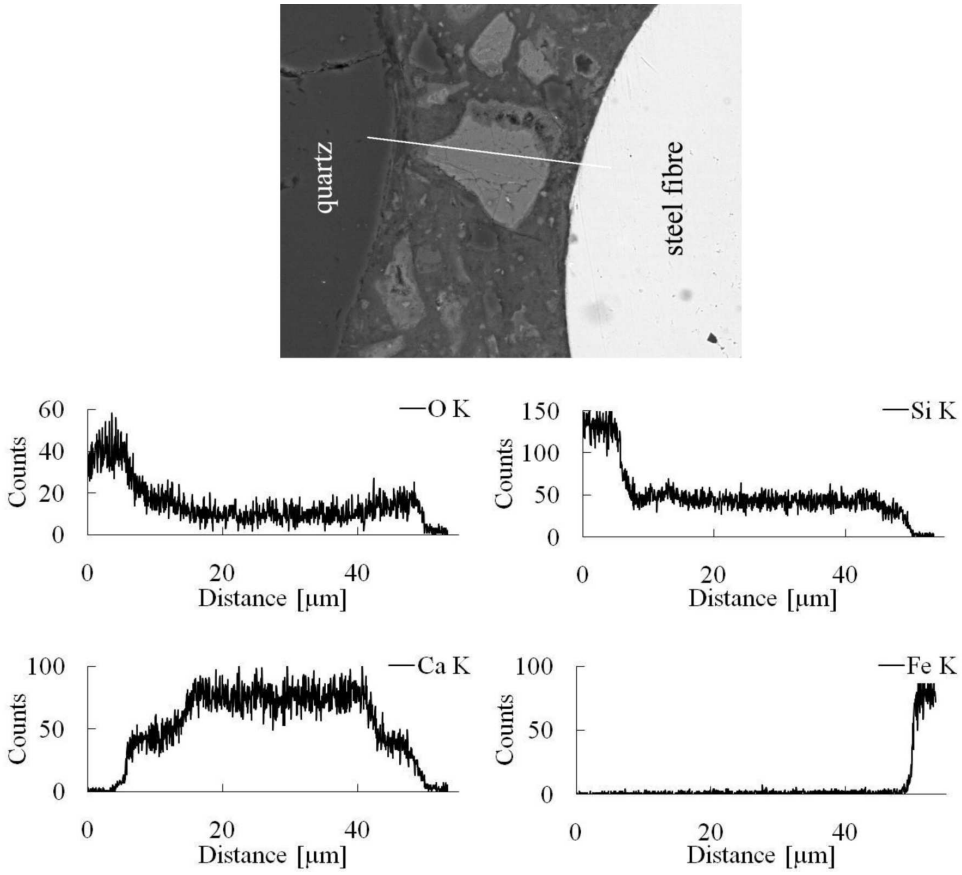

Fig. 11. Transition zone between CSH phase and from the left: quartz grain, relict of cement particle and steel fibre, SEM image with EDS line analysis of autoclaved RPC, magnification 2500x.
Rys. 11. Strefa stykowa pomiędzy fazą CSH oraz od lewej: ziarnem kwarcowym, reliktem ziarna cementu i włóknem stalowym, SEM z liniową analizą EDS autoklawizowanego RPC, powiększenie 2500x

Water absorption was also investigated, however this feature is not suitable for very compacted composites like reactive powder concretes. Regardless of curing conditions the water absorption of designed RPC did not exceed 1.5%. It is worth to notice that autoclaved composites showed the highest absorption, probably because of the presence of xonotlite and tobermorite crystals on the surface of tested specimens.

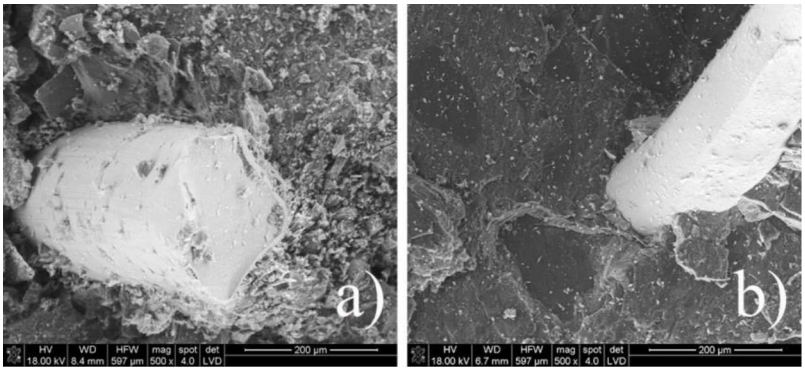

Fig. 12. Steel fibre in RPC, a) curing in water, b) autoclaving, SEM, magnification 500x.
Rys. 12. Włókno stalowe w RPC, a) dojrzewającym w wodzie, b) autoklawizowanym, SEM, powiększenie 500x

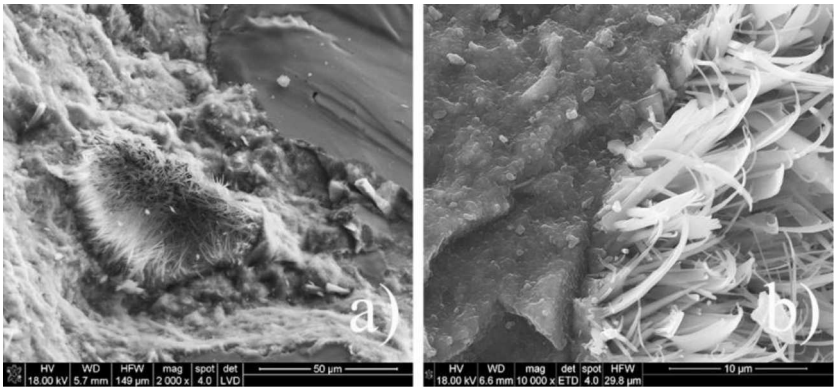

Fig. 13. Partly filled micropore with xonotlite and tobermorite crystals, a) magnification 2 000x, b) magnification 10 000x.
Rys. 13. Mikropor częściowo wypełniony kryształami ksonotlitu i tobermorytu, a) powiększenie 2 000x, b) powiększenie 10 000x

5. Discussion

5.1. Strength and deformability of the RPC during compression

Depending on curing conditions the compressive strength of RPC without fibres vary from 194 to 268 MPa. The lowest value is ascribed to material setting in water, while the highest to autoclaved one. On the basis of results, presented in Table 6, it can be affirmed that steam curing causes increase of compressive strength about 10%, while autoclaving for about 40% in comparison to material setting in water.

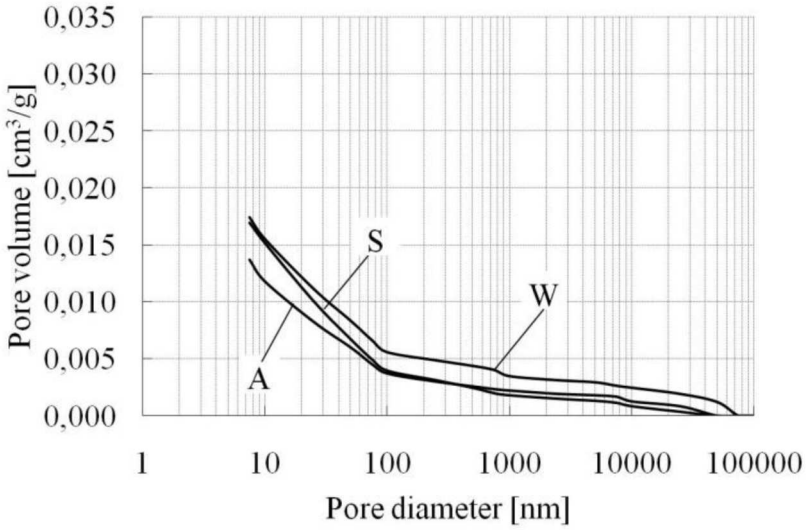

Fig. 14. Pore volume versus pore diameter of RPC matrices cured in water (W), steamed (S), and autoclaved (A).
Rys. 14. Rozkład porowatości matrycy RPC dojrzewającej w wodzie (W), naparzanej (S), oraz autoklawizowanej (A)

Increase of compressive strength of RPC with variable fibres fractions are similar for steam curing as well as autoclaving. The values of compressive strength of RPC with fibres vary from 202 MPa (V_f=0.5% vol. setting in water) to 315 MPa (V_f=4.0% vol. autoclaving). Linear progression of compressive strength versus steel fibres volume fraction can be observed for all studied curing conditions [19].

Moreover it is worth to notice that regardless of curing conditions, the influence of steel fibres content on increase of compressive strength is similar. Only in case of autoclaved RPC containing 2 to 4% vol. of fibres a little in plus deviation can be observed.

On the basis of curves presented in Fig. 5 and values included in table 7, it can be concluded that neither curing conditions nor presence of steel fibres do not influence on parameters characterizing deformability of RPC during compression. Modulus of elasticity vary from 44 to 50 GPa, which corresponds with the values obtained by Fehling et al. [8], however Poisson ratio remain stable on the level 0.20. The smallest value of modulus of elasticity was observed in case of steam–cured composite.

5.2. STRENGTH AND DEFORMABILITY OF THE RPC DURING BENDING

Depending on curing conditions the flexural strength of RPC without fibres ranges from 11 to 19 MPa. As well as in case of compressive strength, above mentioned extreme values are ascribed to setting in water and autoclaving respectively. The steam

curing contributes to 35% flexural strength enhancement, while autoclaving to 75% in comparison to material setting in water.

The flexural strength of RPC with variable amount of fibres vary from 12 MPa (V_f=0.5% vol. setting in water) to 27 MPa (V_f= 4.0% vol. autoclaving). The influence of fibres content on discussed strength is greater than in case of compressive strength. Higher than double increase of flexural strength was observed for RPC cured in water and containing 4% vol. of fibres. In case of steam cured and autoclaved materials with the same amount of fibres the increase of flexural strength was equal to 60 and 45%, respectively. Like in case of compressive strength, the flexural strength for all curing conditions increases in linear rate versus volume fraction of fibres [19].

Opposite to compressive strength test results (Table 6), the influence of hydrothermal treatment on flexural strength of reactive powder concrete versus volume fraction of steel fibres is less distinct.

Work of fracture WF enhances, with increase of steel fibres volume. It is worth to notice that regardless of fibres amount in all considered cases, work of fracture is the highest for autoclaved materials (Fig. 8a). This phenomenon could be explained by two following mechanisms: the first is strengthening of mineral matrix of the composite as a result of hydrothermal treatment at 250°C and the second is the increase of adhesion between matrix and fibres.

Materials that were steamed and cured in water show nearly identical values of fracture toughness indices for whole range of fibres dosage (Fig. 8b,c,d). The maximum value of indices I_5, I_{10} and I_{20} can be observed in composites containing 3% vol. of fibres. Further increase of fibres volume (V_f= 4% vol.) leads to decrease of all determined toughness indices. This effect is ascribed to steamed and cured in water materials, while the autoclaved composites do not reveal such a tendency. This can be attributed to increase of strength of mineral matrix. Calculated fracture toughness indices I_5 and I_{10} suit to results presented by Katz et al. [10]. The authors showed 6,4 and 11,4 values for indices I_5 and I_{10}, respectively. Their specimens had the same dimensions, were cured in natural conditions and contained as much as 9% vol. of steel fibres (6mm in length, 0.16mm in diameter).

In turn, autoclaved reactive powder concretes require relatively high energy to trigger off the first crack in mineral matrix, what entails decrease of all fracture toughness indices up to 3% vol. content of steel fibres.

To the MOR point can be ascribed the highest stress that is carried by included fibres after the first crack of mineral matrix. Therefore increase of f_{MOR}, when volume fraction of steel fibres also increases, seems to be natural phenomenon. In other words, the higher amount of fibres, the higher load can be carried by them. In opposite to f_{MOR}, the f_{LOP} does not increase in whole analyzed range of fibres content. Of course, because of much higher modulus of elasticity of the steel fibres, in comparison to the mineral matrix, actual stress is also carried by them before the first crack is obtained. This could be an explanation of slight increase of the f_{LOP}, until the fibres content reaches 1 or 2% of volume, depending on curing conditions. However higher amount

of dispersed reinforcement brings about decrease of f_{LOP}, which can be ascribed to lower cross–sectional area of the matrix that is subjected to the negative stress.

On the basis of test results presented in Fig. 8e and 8f, steel fibres content, that causes deflection–hardening behavior, can be estimated. In case of samples cured in water and steamed concretes this amount should be about 1.5% vol. However, autoclaved composites remain deflection–softening until the 2.5% of volume fraction (see Fig. 8g).

5.3. MICROSTRUCTURE

It is worth to notice that regardless of later curing conditions, morphology of CSH phase occurred during preliminary setting did not change. Amorphous calcium silicate hydrates synthesized in natural conditions reveal type IV CSH phase, according to Diamond's classification. However, in Fig. 9 increase of compactness of the microstructure during heat treatment can be perceived.

In Fig. 13 it can be observed that crystallization of the xonotlite and tobermorite occurs in empty spaces, where absence of primary, amorphous CSH phase was detected. Thereby, these crystals do not destroy previously created structure, but only fill in pores and microcracks.

Transition zone between steel fibres and CSH phase in reactive powder concrete cured in water, steamed and autoclaved is presented in Fig. 10 and 11. EDS line analysis and observation with magnification 20 000x of the microstructure, allow to state a lack of portlandite crystals in the transition zone in all considered curing conditions.

As regards microporosity measured by mercury porosimetry, the heat treatment of RPC influence on that feature. In case of steamed material no difference in total porosity comparing to composite cured in water can be observed (see Fig. 14). However stem–curing brings about profitable effect i.e. decrease of volume fraction of macropores, greater than 100 nm. Parallely, amount of capillary and gel pores in the range from 100 to 3.7 nm increases.

Autoclaved concretes reveal decrease of porosity in the range of macro, capillary as well as gel pores. This phenomenon can be explained by both increase of pozzolanic reactivity of all components and crystallization of tobermorite and xonotlite in defects of the microstructure. The total porosity of autoclaved concrete decreased about 20% with reference to material cured in water.

6. CONCLUSIONS

The presented test results allow to draw following conclusions:

1) It is possible to receive ultra-high performance concrete using commonly available ingredients and generally traditional curing conditions. In case of material without fibres and cured in natural conditions compressive strength is about 200 MPa and

flexural strength 11 MPa. Application of steam curing allows to increase both stregths up to 212 and 14 MPa, respectively, while autoclaving even to 268 MPa and 18 MPa.

2) Steel fibres addition allows to further increase both compressive as well as flexural strengths. The highest values reached 315 MPa for compressive strength and 27 for flexural strength. These parameters were obtained for autoclaved composite, containing 4% vol. (310 kg/m^3) of steel fibres.

3) Regardless of curing conditions and steel fibres content modulus of elasticity and Poisson ratio remain stable and equals 47 GPa and 0.20, respectively.

4) Concretes cured in water and steam–cured reveal deflection–hardening behavior, if steel fibres content exceed 1.5% vol. In case of autoclaved composite this amount should be more than 2.5% vol.

5) On the basis of presented test results of compressive and flexural strength (Table 6), it can be affirmed that content of examined steel fibres (l = 6mm, ϕ = 0,16 mm) should not exceed 3% of volumetric fraction. Further increase of fibres dosage does not bring significant advantages.

6) Steel fibres content and curing conditions strongly influence deformability of reactive powder concrete in bending test. In order to obtain optimum ductility of tested composites, addition of steel fibres should not exceed 3% vol. It is similar phenomenon which was observed during determination of compressive and flexural strength.

7) Ultra high values of mechanical features of RPC can be ascribed to its microstructure, which is characterized by very compacted texture of CSH phase with superb adhesion to the granular components (i.e. relicts of cement particles and grains of microaggregate) as well as steel fibres. In case of autoclaved composites, crystalline hydrated calcium silicates (xonotlite and tobermorite), which appears in sparse defects of the composite, positively influence its properties.

8) Taking into consideration presented test results; it seems to be purposeful to continue research in order to determine impact of hybrid fibres, with variable length on mechanical properties of RPC.

References

1. P. Acker, M. Behloul, *Ductal technology: a large spectrum of properties, a wide range of application*, International Symposium on Ultra High Performance Concrete, Kessel Germany, 2004, 11-23.
2. ASTM C1018-97 Standard test method for flexural toughness and first-crack strength of fiber-reinforced concrete (using beam with third-point loading), Withdrawn 2006.
3. P. Blais, M. Couture, *Precast, prestressed pedestrian bridge - World's first Reactive Powder Concrete Structure*, PCI Journal IX-X 1999, 60-71.
4. M. Cherezy, V. Maret, L. Frouin, *Microstructural analisis of RPC (Reactive powder concrete)*, Cement and Concrete Research **25**, 1491-1500, 1995.
5. M. Cherezy, V. Maret, L. Frouin, *Microstructural analysis of RPC (Reactive powder concrete)*, Cement and Concrete Research, **25**, 1491-1500, 1995.

6. S. COLLEPARDI, L. COPPOLA, R. TROLI, M. COLLEPARDI, *Mechanical Properties of Modified Reactive Powder Concrete*, American Concrete Institute, **173**, 1-22, 1997.
7. DONG JOO KIM, A.E. NAAMAN, S. EL-TAWIL, *Comparative flexural behaviour of four fiber reinforced cementitious composites*, Cement & Concrete Composites, **30**, 917-928, 2008.
8. E. FEHLING, T. LEUTBECHER, K. BUNJE, *Design relevant properties of hardened Ultra High Performance Concrete*, International Symposium on Ultra High Performance Concrete, Kessel Germany, 327-338, 2004.
9. G. HEROLD, H.S. MÜLLER, *Measurement of porosity of ultra high strength fibre reinforced concrete*, International Symposium on Ultra High Performance Concrete, Kessel Germany, 685-694, 2004.
10. A. KATZ, A. BENTUR, A. DANCYGIER, D. YANKELEVSKY, D. SHERMAN, *Ductility of high performance cementitious composites*, Concrete Science and Engineering. A Tribute to Arnon Bentur, International RILEM Symposium, Evanston, IL, USA, March 2004, 117-127.
11. A.M. NEVILLE, Właściwości betonu, Polski Cement, Kraków 2000.
12. M. ORGASS, Y. KLUG, *Fibre Reinforced Ultra-High Strength Concrete*, International Symposium on Ultra High Performance Concrete, Kessel Germany, 637-647, 2004.
13. S. PHILIPPOT, S. MASSE, H. ZANNI, P. NIETO, V. MARET, M. CHEYREZY, *29Si NMR study of hydratation and pozzolanic reactions in reactive powder concrete (RPC)*, Magnetic Resonanse Imaging, **14**, 891-893, 1996.
14. PN – EN 14580, Natural stone test methods – Determination of static elastic modulus.
15. P. RICHARD, M. CHEYREZY, *Composition of Reactive Powder Concrete*, Cement and Concrete Research, **25**, 7, 1501-1511, 1995.
16. S. STAQUET, B. ESPION, *Early age autogenous shrinkage of UHPC incorporating very fine fly ash or metakaolin in replacement of silica fume*, International Symposium on Ultra High Performance Concrete, Kessel Germany, 2004, 587-599.
17. S. STAQUET, B. ESPION, *Influence of Cement and Silica Fume Type on Compressive Strength of Reactive Powder Concrete*, 6th International Symposium on High Strength /High Performance Concrete, Leipzig, June 2002, 1421-1436.
18. H. ZANNI, M. CHEYREZY, V. MARET, S. PHILIPPOT, P. NIETO, *Investigation of hydration and pozzolanic reaction in reactive powder concrete (RPC) using 29Si NMR*, Cement and Concrete Research, **26**, 93-100, 1996.
19. T. ZDEB, J. ŚLIWIŃSKI, *Effect of curing conditions and steel fiber addition on the compressive and flexural strength of reactive powder concrete* (in Polish), Inżynieria i Budownictwo, **12**, 693-697, 2008.
20. T. ZDEB, *The influence of composition and production technology on selected properties of reactive powder concretes*, PhD thesis (in Polish), Cracow University of Technology, 2010.

WPŁYW WYBRANYCH CZYNNIKÓW MATERIAŁOWYCH I TECHNOLOGICZNYCH NA WŁAŚCIWOŚCI MECHANICZNE I MIKROSTRUKTURĘ BETONÓW Z PROSZKÓW REAKTYWNYCH (BPR)

Streszczenie

Artykuł dotyczy charakterystyki wybranych właściwości i mikrostruktury Betonów z Proszków Reaktywnych (BPR), wytworzonych w Politechnice Krakowskiej. Analizie poddano wpływ trzech warunków

dojrzewania: dojrzewanie w wodzie (W), naparzanie niskoprężne (S) oraz autoklawizacja (A), a także zawartości włókien stalowych na wybrane właściwości BPR. Kompozyt charakteryzował się stałym współczynnikiem wodno-spoiwowym 0,20 oraz zawartością pyłu krzemionkowego 20% w stosunku do masy cementu. W zależności od warunków dojrzewania i udziału włókien wytrzymałość na ściskanie wahała się w granicach od 200 do 315 MPa, natomiast moduł sprężystości wyznaczany podczas ściskania wynosił około 50 GPa. Podczas trzypunktowego zginania beleczek RPC rejestrowano zależność siła-ugięcie, na podstawie której wyznaczono następujące parametry: wytrzymałość na rozciąganie przy zginaniu, wartość naprężenia w punktach LOP i MOR (opis w tekście), energię zniszczenia WF oraz wartości współczynników toughness indices I_5, I_{10} and I_{20}. Zarówno udział włókien stalowych jak i warunki dojrzewania BPR mają wpływ na odkształcalność kompozytu podczas próby zginania.

Remarks on the paper should be sent to the Editorial Office no later than September 30, 2011

Received December 10, 2010 revised version June 6, 2011